Journal of Marine Research, 52, 219–238, 1994

Modelling the effect of physical variability on the midwater chlorophyll maximum

by Jonathan Sharples[1,2] and Paul Tett[1]

ABSTRACT

A coupled model, employing turbulence closure physics and cell-quota threshold limitation biology, has been used to simulate the evolution of the vertical distribution of phytoplankton in a seasonally stratified shelf sea. Predictions are compared with observations from the North Sea. Variations in surface wind stress, which episodically weaken the thermocline barrier to nutrient input to the photic zone, are shown to make an important contribution to the formation of a midwater chlorophyll maximum in Summer.

1. Introduction

Increasing understanding of the physics of shelf seas has led to the hypothesis that regional distributions and seasonal cycles of phytoplankton can be explained in terms of the relationship between vertical mixing and the requirements of planktonic micro-algae for light and nutrients (Pingree *et al.,* 1977). Numerical simulation offers one method of testing this hypothesis. Several authors have used models driven by vertical turbulent diffusion to simulate vertical distributions of phytoplankton biomass in particular seasons, deriving values of diffusion coefficients from observed temperature profiles. In shelf sea regions these include Fasham *et al.* (1983) and Tett (1981) with similar work by Jamart *et al.* (1977) and Taylor *et al.* (1986) focusing on the surface mixed layer of the deep ocean. Investigating seasonal cycles through simulation is a more demanding task, requiring coupled physical-biological models that generate vertical distributions of photosynthetically active radiation (PAR), as well as of mixing, from meterological and tidal data. Woods and Tett (1994) and Tett *et al.* (1993) used boundary layer approximations: conservation rules for potential energy and heat were used to predict the depth of the thermocline separating well-mixed surface and bottom boundary layers, thus defining the light-climate for phytoplankton. These models transfer nutrients from the bottom to the surface layer by entrainment rather than Fickian diffusion. They successfully predict the main

1. University of Wales, Bangor, School of Ocean Sciences, Menai Bridge, Gwynedd, LL59 5EY, United Kingdom.

2. Present address: New Zealand Oceanographic Institute, Greta Point, Evans Bay Parade, P.O. Box 14-901, Kilbirnie, Wellington, New Zealand.

blooms observed in the surface layer in the North Sea, but cannot simulate the other characteristic feature of the phytoplankton biology of seasonally-stratified shelf seas, which is the existence of a mid-water chlorophyll maximum during much of the summer. Simple "light-nutrient-mixing" theory explains this maximum as the result of the vertical (and diapycnal) diffusion of nutrients into the thermocline, which provides a midwater region of low (but not zero) vertical mixing within the euphotic zone. Other explanations have included depth-dependent phytoplankton sinking rates (Steele and Yentsch, 1960), depth-dependent ratios of algal chlorophyll to cellular nutrient (Kiefer and Kremer, 1981), nutrient-controlled dinoflagellate vertical migration (Tett, 1987) and isopycnal diffusion from an adjacent mixing zone (Simpson *et al.,* 1982).

In this paper we present results from a physical-biological model that can simulate the midwater maximum. The physical submodel uses a level 2 turbulence closure scheme (after Mellor and Yamada, 1974, 1982) to calculate the seasonal evolution of depth-varying vertical diffusivities. Walters (1980) followed a similar approach in modelling seasonal algal growth in a lake using an empirical relationship between vertical eddy diffusivity and stability, while more recently Varela *et al.* (1992) have used the same level 2 turbulence closure scheme in a study of steady state biological conditions in the ocean surface mixed layer.

The biological submodel applies the cell-quota, threshold-limitation scheme of Tett *et al.* (1986), with phytoplankton biomass defined by chlorophyll and nitrogen. We use the test of predicting a realistic midwater maximum in chlorophyll as a means of examining detailed hypotheses about physical-biological interactions. This leads to the conclusion that the existence of a chlorophyll maximum has important implications for understanding the nature of mixing in the thermocline. Finally, the model is used to demonstrate important differences between forcing with time-averaged, and with raw, meteorological data.

2. Background to the physical model

The model is one dimensional, calculating conditions through the depth of the water column. The depth is split into a number of discrete depth cells of constant size, Δz, so that $n = h/\Delta z$ where n is the number of depth cells and h is the total depth. Velocities and scalars are associated with the center of a depth cell, while coefficients of eddy viscosity and diffusivity are calculated at the boundaries between depth cells (see Fig. 1).

The equations of motion in the two horizontal directions are:

$$\frac{\partial u}{\partial t} = -A_x \sin(\omega t - \phi_x) + fv + \frac{\partial}{\partial z}\left(N_z \frac{\partial u}{\partial z}\right) \tag{1}$$

$$\frac{\partial v}{\partial t} = -A_y \sin(\omega t - \phi_y) - fu + \frac{\partial}{\partial z}\left(N_z \frac{\partial v}{\partial z}\right) \tag{2}$$

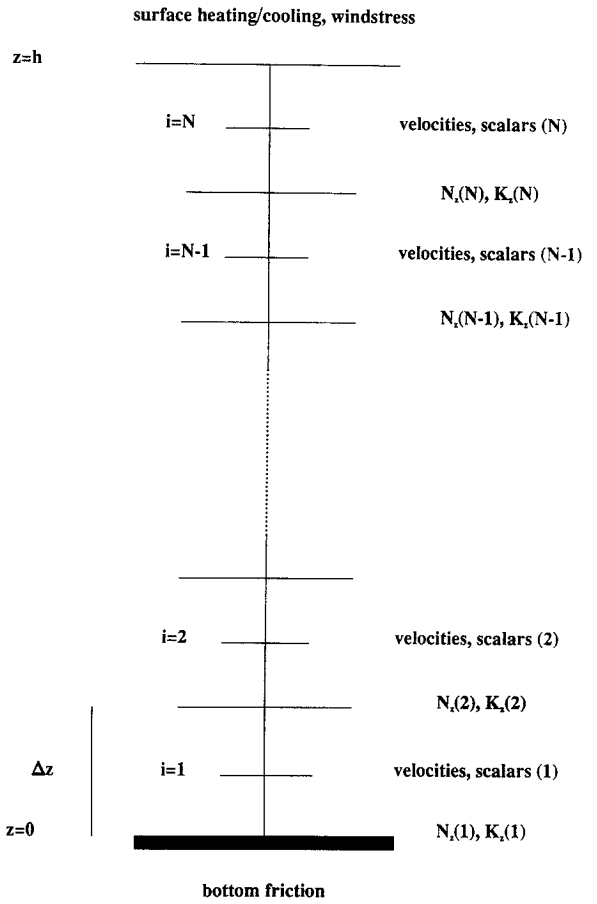

Figure 1. Schematic representation of the model grid. Velocities and scalars (temperature, salinity, biomass, algal nitrogen, and inorganic nitrogen) are associated with the center of each depth cell. Gradient Richardson numbers are calculated at the boundaries between cells, leading to values for N_z and K_z.

with x positive eastward, y positive northward, and z increasing from zero at the seabed to h at the sea surface. The first term on the right of Eqs. (1) and (2) represents the oscillating pressure gradient responsible for driving the tidal currents, with $A_{x,y}$ the tidal surface slope amplitudes (multiplied by g, the gravitational acceleration) and $\phi_{x,y}$ the tidal slope phases in the x and y directions, and ω the tidal frequency. The second term is due to inertial forcing by the earth's rotation, with f the Coriolis parameter, and the third describes the transport of momentum through the water column via frictional coupling between the layers in terms of the vertical eddy viscosity, N_z. The boundary condition for stress at the seabed is

$$\tau_x = -k_b\rho(u_1^2 + v_1^2)^{1/2}u_1; \qquad \tau_y = -k_b\rho(u_1^2 + v_1^2)^{1/2}v_1 \tag{3}$$

with u_1 and v_1 the near-bottom x and y components of current velocity, ρ the water density, and k_b the quadratic friction coefficient (≈ 0.003). Windstress is applied at the surface via

$$\tau_{sx} = k_s \rho_a (u_w^2 + v_w^2)^{1/2} u_w; \qquad \tau_{sy} = k_s \rho_a (u_w^2 + v_w^2)^{1/2} v_w \tag{4}$$

with u_w and v_w the x and y components of the wind velocity, ρ_a the air density (1.2 kg m^{-3}), and k_s a surface quadratic drag coefficient (≈ 0.0014).

Eqs. (1) and (2) are integrated forward through time explicitly, which puts a stability constraint on the time step of the model of

$$\Delta t \leq \frac{(\Delta z)^2}{2N_z} \tag{5}$$

where N_z is the maximum value attained by the eddy viscosity (Press *et al.,* 1986).

Density changes within the water column are brought about by surface heating and cooling with the vertical turbulent transfer of heat (density) controlled by

$$\frac{\partial T}{\partial t} = \frac{\partial}{\partial z}\left(K_z \frac{\partial T}{\partial z}\right) \tag{6}$$

where T is the temperature and K_z is the coefficient of vertical eddy diffusivity. There is no flux of heat through the seabed, and no flux of salt through either the seabed or the sea surface. Surface heating within the model follows the approach of Simpson and Bowers (1984) (after Edinger *et al.,* 1968), and requires meteorological inputs of solar radiation (Q_s/W m^{-2}), dewpoint temperature (T_d/°C), and wind speed (w/m s^{-1}). The net heat input, Q, is given by

$$Q = Q_s + k(T_d - T_s) \tag{7}$$

with T_s the surface temperature and

$$k = 4.5 + 0.05T_s + (\beta + 0.47)f(w) \tag{8}$$

$$\beta = 0.35 + 0.015T_m + 0.0012T_m^2 \tag{9}$$

$$T_m = 0.5(T_s + T_d) \tag{10}$$

$$f(w) = 9.2 + 0.46w^2 \tag{11}$$

The term involving k in Eq. (7) represents a heat loss rate and is applied to the surface element of the model grid. The solar heat component of Q is then distributed exponentially through the water column via the relation

$$\frac{\partial Q_s(z)}{\partial z} = -Q_s(z)(\lambda_0 + \epsilon X(z)) \tag{12}$$

with λ_0 the attenuation coefficient (0.1 m^{-1}). The term ϵX represents the effect of the increase in water opacity caused by the biomass, with $\epsilon = 0.012$ m^2 (mg chl)$^{-1}$ and $X(z)$ the local phytoplankton biomass (mg chl m^{-3}).

The essential interaction between vertical transfer by turbulent processes and water column structure is represented in terms of a Mellor-Yamada level 2 closure scheme (see Mellor and Yamada, 1974, 1982) which determines the eddy coefficients of viscosity and diffusivity from the local gradient Richardson number. The level 2 approach assumes a local equilibrium between production and dissipation of turbulent kinetic energy, described by an energy equation of the form

$$N_z\left[\left(\frac{\partial u}{\partial z}\right)^2 + \left(\frac{\partial v}{\partial z}\right)^2\right] + K_z\left(\frac{g}{\rho}\frac{\partial \rho}{\partial z}\right) = \frac{q^3}{B_1 l} \tag{13}$$

where B_1 is an empirically determined constant of the closure scheme, and q is the turbulent intensity (m s^{-1}). The turbulent lengthscale, l, we describe by

$$l(z) = \kappa z\left(1 - \frac{z}{h}\right)^{1/2} \tag{14}$$

with z the height above the seabed and $\kappa = 0.41$ is von Karman's constant. Eq. (13) represents an equilibrium between shear production and buoyancy production of turbulent kinetic energy on the left hand side, and disspation on the right.

The closure scheme allows calculation of N_z and K_z at each element in the model grid in terms of the local stability, the turbulent lengthscale, and the turbulent intensity via

$$N_z = S_M l q; \qquad K_z = S_H l q \tag{15}$$

where S_M and S_H are stability functions ultimately calculated from the local gradient Richardson number, R_i, via the local flux Richardson number, R_f, through the following set of equations:

$$R_i = -\frac{g(\Delta\rho/\Delta z)}{\rho(\Delta U/\Delta z)^2} \tag{16}$$

$$R_f = \tfrac{1}{2}[R_{f1} + R_i R_{f1} R_{f2}^{-1} - ((R_{f1} + R_i R_{f1} R_{f2}^{-1})^2 - 4R_{f1}R_i)^{1/2}] \tag{17}$$

$$S_M = B_1^{-1/3}\frac{(1 - R_{fc}^{-1}R_f)(1 - R_{f1}^{-1}R_f)}{(1 - R_f)(1 - R_{f2}^{-1}R_f)}; \qquad S_H = \frac{B_1^{-1/3}}{P_r^N}\frac{(1 - R_{fc}^{-1}R_f)}{(1 - R_f)}. \tag{18}$$

Here $\Delta\rho/\Delta z$ is the vertical density gradient and $\Delta U/\Delta z$ the vertical velocity gradient between adjacent depth elements. R_{fc}, R_{f1}, and R_{f2} are all laboratory determined constants, and P_r^N is turbulent Prandtl number. The values used for the constants

Table 1. Constants required by the biological submodel.

Constant	Units	Description	Value
μ_m	day^{-1}	Maximum specific growth rate	1.2
k_Q	mmol N (mg chl)$^{-1}$	Subsistence quota	0.2
α	mg C (mg chl)$^{-1}$ day^{-1} (W m^{-2})$^{-1}$	Maximum quantum yield	4.1
r^B	mg C (mg chl)$^{-1}$ day^{-1}	Respiration rate	3.5
q^{chl}	mg chl (mg C)$^{-1}$	Cell chl:carbon ratio	0.02
g	day^{-1}	Grazing impact rate	0.12
u_m	mmol DIN (mg chl)$^{-1}$ day^{-1}	Maximum nutrient uptake rate	2.0
Q_m	mmol N (mg chl)$^{-1}$	Maximum cell quota	1.0
k_u	mmol DIN m^{-3}	Nutrient concentration for half maximum uptake	0.3
e	—	Recycled proportion of grazed nutrient	0.5
f_r	day^{-1}	Benthic nutrient input rate	0.02
S_b	mmol DIN m^{-3}	Maximum near-bed DIN concentration	5.0
ϵ	m^2 (mg chl)$^{-1}$	Pigment absorption cross-section	0.012
λ_0	m^{-1}	Attenuation coefficient	0.1

required by the turbulence closure scheme are:

$$B_1 = 15.0; \qquad R_{fc} = 1/6; \qquad R_{f1} = 1/4; \qquad R_{f2} = 1/5; \qquad P_r^N = 1.0. \tag{19}$$

Although algebraically complex, the level 2 closure scheme is straightforward to implement within the model, requiring only the calculation of the profile of the gradient Richardson number to produce the vertical structure of turbulent kinetic energy and the coefficients of eddy viscosity and diffusivity.

3. Background to the biological model

The framework for the biological part of the numerical model follows Tett *et al.* (1986) and Tett (1987). There are four depth and time dependent state variables: phytoplankton biomass (X/mg chl m^{-3}), dissolved inorganic nitrogen (S/mmol DIN m^{-3}), algal internal nutrient (N/mmol N m^{-3}), and PAR (I/W m^{-2}). Constants required by the biological model are listed in Table 1.

(1) X (mg chl m^{-3}), phytoplankton biomass:

$$\frac{\partial X}{\partial t} = \frac{\partial}{\partial z}\left(K_z \frac{\partial X}{\partial z}\right) + \mu X - gX. \tag{20}$$

The first term on the right of Eq. (9) describes the vertical movement of biomass due to turbulent eddy diffusion. The second term is the growth of phytoplankton, with μ the specific growth rate (s^{-1}), given by the either

$$\mu = \mu_m(1 - k_Q/Q) \tag{21}$$

for nutrient determined growth, or

$$\mu = q^{chl}(\alpha \bar{I} - r^B) \tag{22}$$

for light determined growth. Q is the cell quota ($=N/X$) and $\bar{I}$ is the layer mean PAR (W m^{-2}). By taking the lesser of these two possible rates the model simulates growth limitation by either the local PAR or the phytoplankton internal nutrient. The third term represents a sink of biomass resulting from grazing by zooplankton, with g the grazing impact (typically 0.12 day^{-1}). Grazing is only allowed to take place within the model if the biomass is greater than a threshold value (0.1 mg chl m^{-3}), simulating the observed behavior of zooplankton in only feeding when it is energetically favorable to do so.

(2) N (mmol N m^{-3}), algal nitrogen:

$$\frac{\partial N}{\partial t} = \frac{\partial}{\partial z}\left(K_z \frac{\partial N}{\partial z}\right) + uX - gN. \tag{23}$$

This is similar in structure to Eq. (20), though with the term uX representing uptake of nutrient by the phytoplankton. The uptake rate of dissolved inorganic nitrogen, u (mmol DIN(mg chl)$^{-1}$s^{-1}), is a Michaelis-Menten function of the external concentration S of DIN and of the algal internal nutrient quota, Q, given by

$$u = \left[u_m\left(1 - \frac{Q}{Q_m}\right)\frac{S}{(k_u + S)}\right] + (\mu Q{:}\mu < 0; \quad 0{:}\mu \geq 0). \tag{24}$$

DIN is taken up by the phytoplankton up to a maximum value of Q. The method allows for "luxury" uptake of nutrient by the phytoplankton above the immediate requirements for growth. Zooplankton grazing of the nitrogen component of the phytoplankton is represented by the term gN.

(3) S (mmol DIN m^{-3}), dissolved inorganic nitrogen:

$$\frac{\partial S}{\partial T} = \frac{\partial}{\partial z}\left(K_z \frac{\partial S}{\partial z}\right) - uX + egN. \tag{25}$$

Again this is similar to Eqs. (20) and (23). The term uX is a sink for S, removing the nutrient uptake from the surrounding inorganic nitrogen. egN describes the recycling of nutrient grazed by the zooplankton, with e the recycled proportion of grazed nutrient. Nutrient input at the bottom boundary, by resuspended sediments, is modelled by a boundary condition of the form

$$input = f_r(S_b - S_1)n\Delta t \tag{26}$$

where n is the number of depth elements in the model, f_r is an input rate, S_b is an assumed maximum value of near bed DIN, and Δt is the time step.

(4) I (W m^{-2}), photosynthetically active radiation:

$$\frac{\partial I}{\partial z} = -I(\lambda_0 + \epsilon X). \tag{27}$$

This is identical to Eq. (12), but describes attenuation of PAR with depth. The surface boundary condition assumes that 25% of the incident solar radiation is available for photosynthesis, i.e. $I = 0.25\ Q_s$ at the surface.

Each of the state variables is associated with the center of a depth cell within the model framework of Figure 1. A detailed discussion of the equations and empirical constants forming the biological model can be found in the references cited at the beginning of this section.

4. Initial results from the model over a seasonal cycle

The behavior of the model over a seasonal cycle can be illustrated by driving it with average seasonally varying meteorological conditions, as used in Simpson and Bowers (1984), and an M_2 tidal constituent amplitude below the critical strength required to maintain a vertically mixed water column throughout the year. The physical driving parameters for all model runs are summarized in Table 2.

The history of thermal stratification, net surface heat input, surface biomass, and surface DIN are shown in Figure 2. The modelled water column begins to stratify shortly after the vernal equinox, reaching a maximum stability in August. The stratification is then eroded as the net surface heat flux decreases and becomes negative, so that tidal mixing and convective overturning result in a vertically mixed water column by the middle of November. The surface biomass shows the well-documented behavior of a strong bloom in spring just as the water column begins to stratify, with the increasing stability holding an amount of phytoplankton and nutrient up in the photic zone allowing rapid phytoplankton growth until limited by the reduction in the surface nutrients. As the thermocline is weakened in autumn, another smaller bloom occurs until the water column is vertically homogeneous and the phytoplankton respiration rate (r^B in Eq. (22)) exceeds photosynthesis.

The time and depth variation of this cycle is illustrated in depth versus time contour plots of temperature, biomass, and DIN in Figure 3. The confinement of the blooms to the surface layer is clear, as is the effect of the thermocline in preventing nutrient from the bottom layer reaching the surface.

5. The midwater chlorophyll maximum

A comparison of this modelled data with, for instance, the observations of Holligan and Harbour (1977) shows that, while the model is successful in producing the spring and autumn blooms, it is not producing a mid-water maximum in chlorophyll during the stratified period. Such maxima are commonly observed at the

Table 2. Physical driving parameters used for the three model runs.

Parameter	Description	Run 1	Run 2	Run 3
h	Depth (m)	80	80	80
A_x	M_2 surface slope amplitude in x direction (m s^{-2})	4.0×10^{-5}	4.0×10^{5}	4.0×10^{-5}
A_y*	M_2 surface slope amplitude in y direction (m s^{-2})	3.4×10^{-5}	3.4×10^{-5}	3.4×10^{-5}
K_b	Bottom quadratic drag coefficient	0.003	0.003	0.003
K_s	Surface quadratic drag coefficient	0.0014	0.0014	0.0014
w	Wind speed (m s^{-1})	seasonal**	seasonal**	daily mean***
T_d	Dewpoint temperature (°C)	seasonal**	seasonal**	daily mean***
Q	Solar radiation (W m^{-2})	seasonal**	seasonal**	daily mean***
N_{z0}, K_{z0}	Background eddy viscosity and diffusivity (m^2 s^{-1})	0.0	1.0×10^{-5}	0.0
ϕ	Latitude	55N	55N	55N
N	Number of model depth steps	20	20	20
Δt	Model time step (hours)	0.01	0.01	0.01

*Amplitude and phase in the y direction are chosen to produce a degenerate tidal current ellipse. S_2 amplitudes are 30% of the M_2 amplitudes.

**Seasonal mean meteorological forcing (ω_y is the seasonal frequency, phases are relative to March 1st):

$w = 7.1 + 2.2 \sin(\omega_y t + 2.356)$ m s^{-1}
$T_d = 8.85 + 5.07 \sin(\omega_y t - 1.192)$ °C
$Q = 130.0 + 109.0 \sin(\omega_y t - 0.351)$ W m^{-2}

***Daily mean meteorological forcing taken from meteorological model predictions.

base of the thermocline during summer, and a number of hypotheses have been put forward to explain them. These hypotheses can be investigated within the present model framework. Note that the depth-dependent algal chlorophyll to cellular nutrient ratio used by Kiefer and Kremer (1981) cannot be tested within the present biological model framework.

(1) Pingree *et al.* (1977). A slow diapycnal leakage of nutrient into the thermocline, coupled with the relatively long residence times of phytoplankton within that region, can lead to enhanced productivity. This can be incorporated in the model by specifying a lower limit, or "background" level, to the vertical eddy viscosity and diffusivity below which they are not allowed to fall, i.e.

$$N_z, K_z \geq \textit{background}. \tag{28}$$

(2) Steele and Yentsch (1960). Phytoplankton sinking rates may decrease as the nutrient supply increases, allowing them to take advantage of higher ambient nutrient levels near the thermocline. We model this by applying an additional term

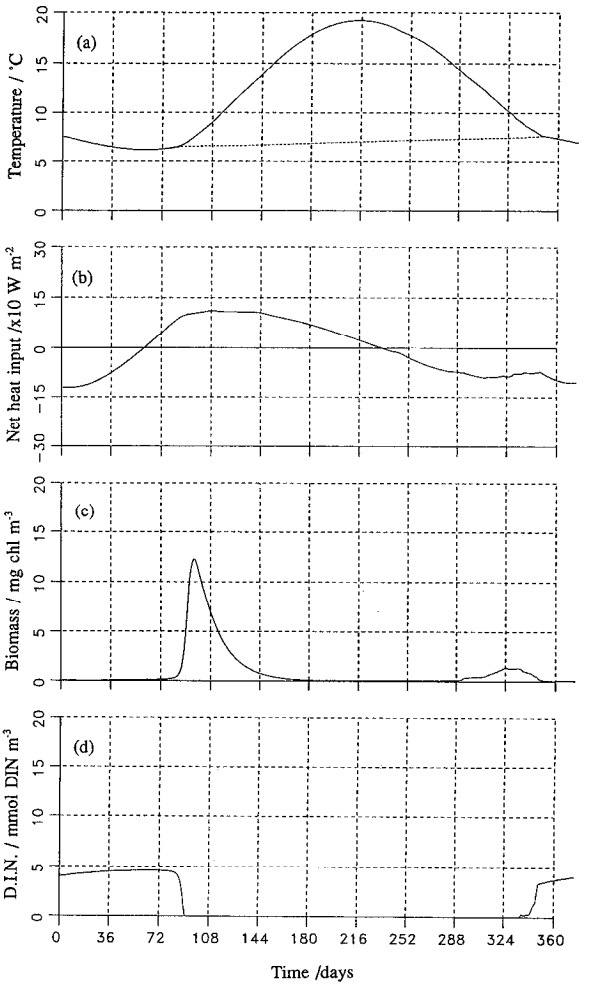

Figure 2. Basic modelled stratification and primary production over a seasonal cycle (run 1). Day 0 corresponds to January 1st. (a) Surface and bottom temperatures (°C) versus time (days). The solid line is the surface temperature, the broken line is the bottom temperature; (b) Net surface heat input ($\times 10$ W m^{-2}) versus time (days); (c) Surface biomass (mg chl m^{-3}) versus time (days); (d) Surface dissolved inorganic nitrogen (mmol DIN m^{-3}) versus time (days).

describing a constant sinking rate to Eqs. (20) and (23) of

$$\frac{\partial(X, N)}{\partial t} = -w_s \frac{\partial(X, N)}{\partial z} \tag{29}$$

where $w_s = 1.0$ m day^{-1} within the surface mixed layer, and $w_s = 0.0$ m day^{-1} at and below the thermocline.

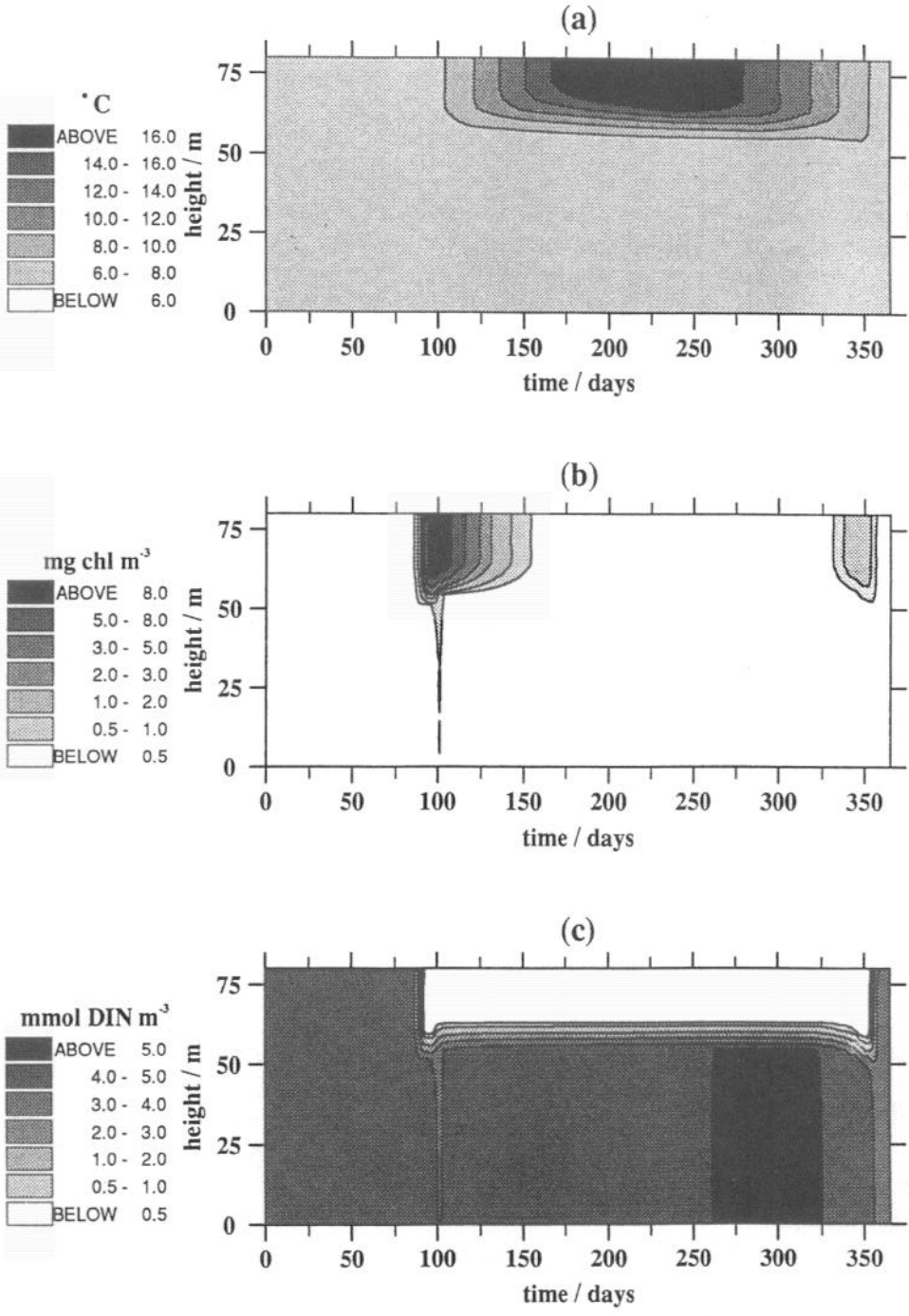

Figure 3. Height (meters) versus time (days) contour plots of: (a) temperature (°C); (b) biomass (mg chl m^{-3}); (c) DIN (mmol DIN m^{-3}); over a seasonal cycle (run 1).

(3) Margalef (1978), Tett (1987). Dinoflagellates and diatoms may migrate upward toward the light when replete with nutrients, and downward when nutrient deficient, suggesting that they can migrate below the thermocline to gather nutrient and then return to the photic zone. We parameterize this again with Eq (29), but with w_s ranging from $+5.0$ m day^{-1} for $Q = Q_m$ to -5.0 m day^{-1} for $Q = 0.0$. Thus as the cell nutrient quota tends toward the maximum Q_m the cells migrate upward toward higher PAR levels, and as internal nutrients are utilized and Q decreases they migrate downward toward higher DIN levels. At $Q = k_q$, the subsistence cell quota, $w_s = 0.0$ m day^{-1}.

By experimenting with each of these hypotheses within the model we found that the only way to achieve a mid-water maximum in chlorophyll was by the use of the background mixing of hypothesis (1) above. While the other hypotheses do alter the exact structure of any mid-water maximum when operating at the same time as this background mixing, they are not individually capable of producing higher productivity within the thermocline. Figure 4 demonstrates the effect of employing a background diffusivity of 1.0×10^{-5} m^2 s^{-1} in a model run otherwise identical to that illustrated in Figure 3.

We suggest, then, that without this background viscosity the turbulence closure scheme produces thermocline structure that is too stable, preventing any connection between the surface and bottom layers. The observed existence of mid-water maxima of biomass implies that such complete decoupling of the two layers does not occur. The value of the background mixing that we have used is similar to that used by, for instance, Mellor and Durbin (1975) and Chen *et al.* (1988) in models employing similar closure schemes.

6. Comparison between model and observations

A more-rigorous test of the model can be made by using an appropriate data set that has well defined tidal and meteorological conditions. For this we use temperature and fluorescence data from a series of monthly C.T.D. surveys taken as part of the U.K. North Sea Project. Station CS (latitude 55°C 30′N, longitude 0° 55′E), situated in a region of the North Sea that stratifies during the summer months, was chosen for the comparison. Temperature and chlorophyll structure over the seasonal cycle was observed by a series of monthly C.T.D. casts, while the strengths of the tidal current constituents were measured from a current meter mooring deployment at the position. Daily averages of wind speed and dewpoint temperature were available from the U.K. Meteorological Office numerical model, and daily means of solar radiation were taken from observations at a nearby meteorological station.

Figure 5 illustrates the history of the temperature and chlorophyll at station CS over the period October 1988 to September 1989 (Howarth *et al.,* 1993). Maximum values of biomass were associated with the onset of stratification in spring, and the breakdown of stratification in the following autumn. There was also evidence for a

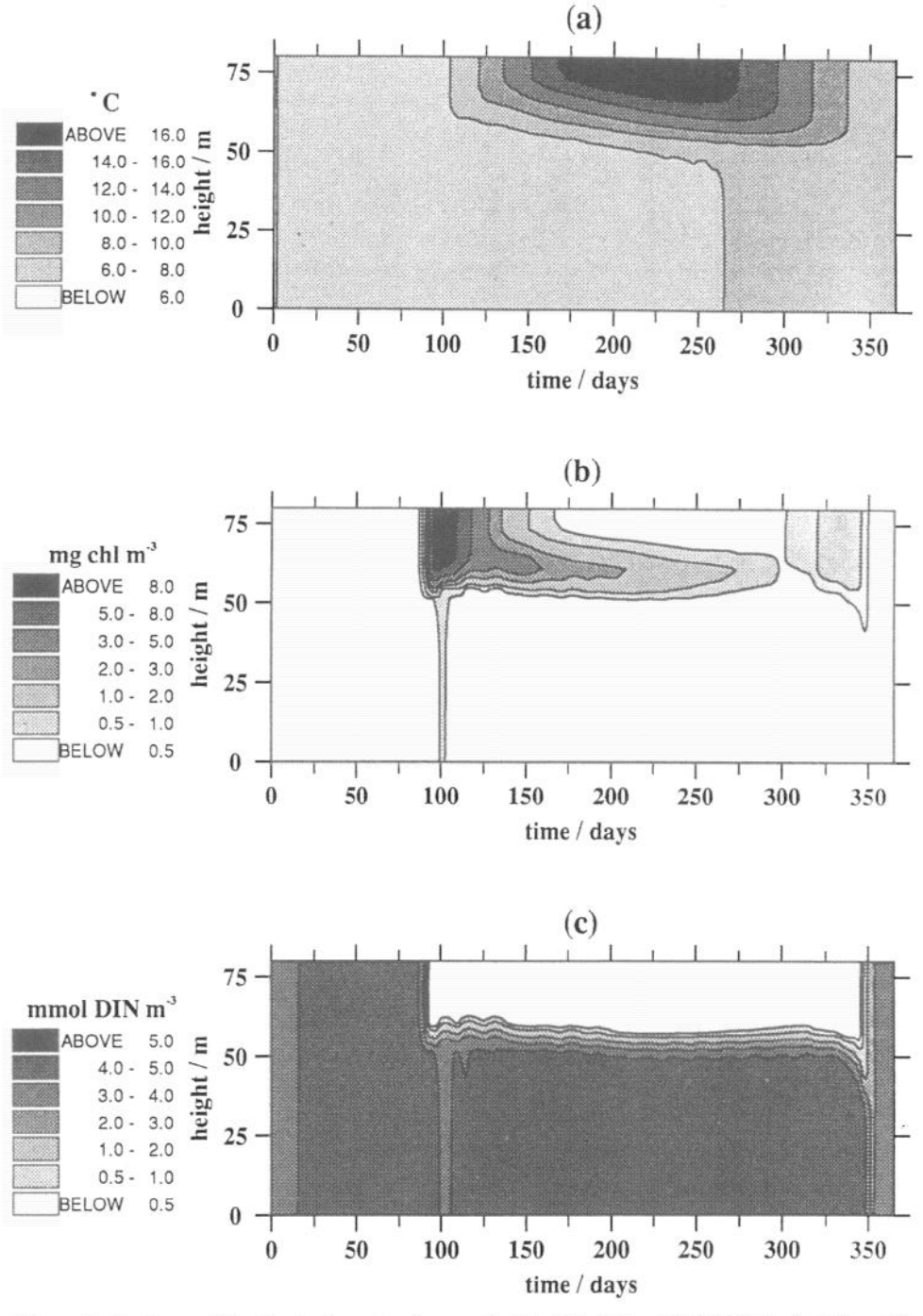

Figure 4. As Figure 3, but including a background eddy diffusivity of 1.0×10^{-5} m^2 s^{-1} (run 2).

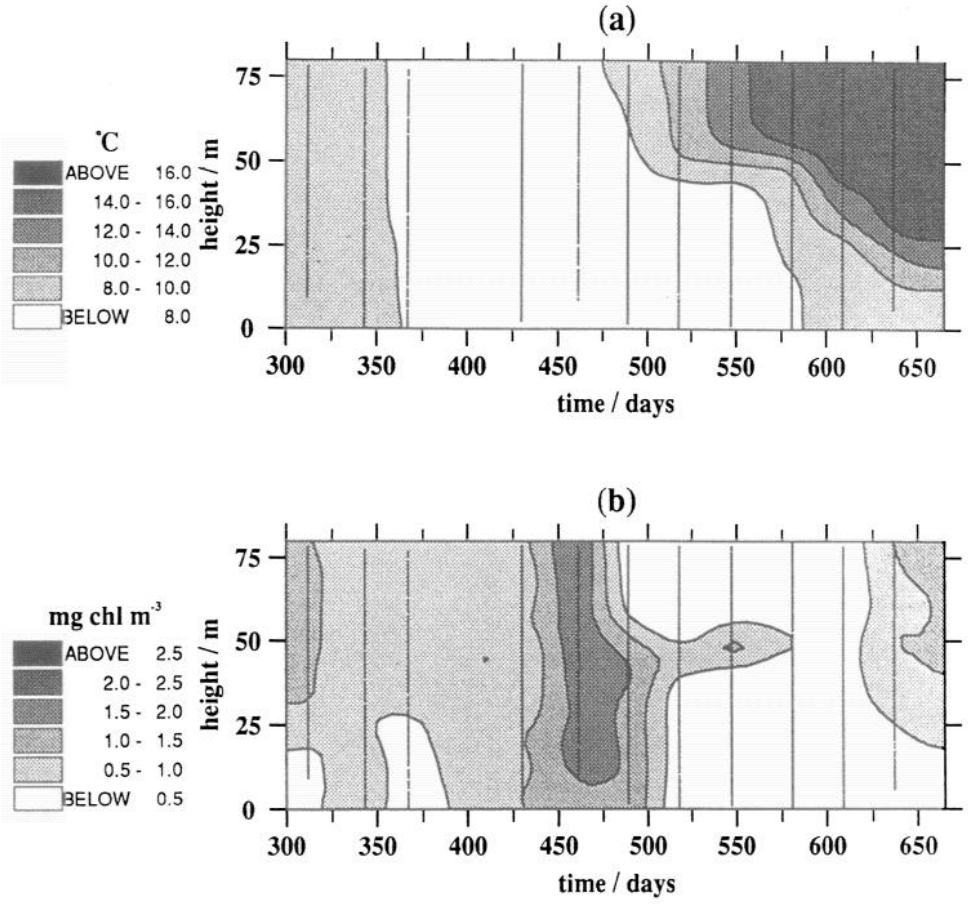

Figure 5. C.T.D. observations made at station CS in the North Sea. Julian day 0 is January 1st 1988, Julian day 300 corresponds to October 26th 1988. Height (meters) versus time (days) contours of: (a) temperature (°C); (b) biomass (mg chl m^{-3}). Vertical lines mark the times and vertical extent of the C.T.D. casts.

midwater chlorophyll maximum at the thermocline between these two periods of high production. It must be noted, however, that the interval of about a month between successive C.T.D. casts results in some uncertainty concerning the temporal extent of patches in chlorophyll. Also, the spring bloom is known to have occurred between the two cases at days 461 and 489, and so it is not represented in Figure 5. A fluorometer moored at 18 m below the surface recorded surface-layer chlorophyll reaching a maximum of about 8 mg chl m^{-3} on April 23rd (day 478), with an initial peak of about 2 mg chl m^{-3} on April 12th (day 467) (Mills and Tett, 1990; Mills *et al.*, 1993).

The corresponding model data, from a run using the daily meterological inputs and without any background mixing and using M_2 and S_2 tidal constituent amplitudes measured by the current meter mooring, are shown in Figure 6 with the addition of

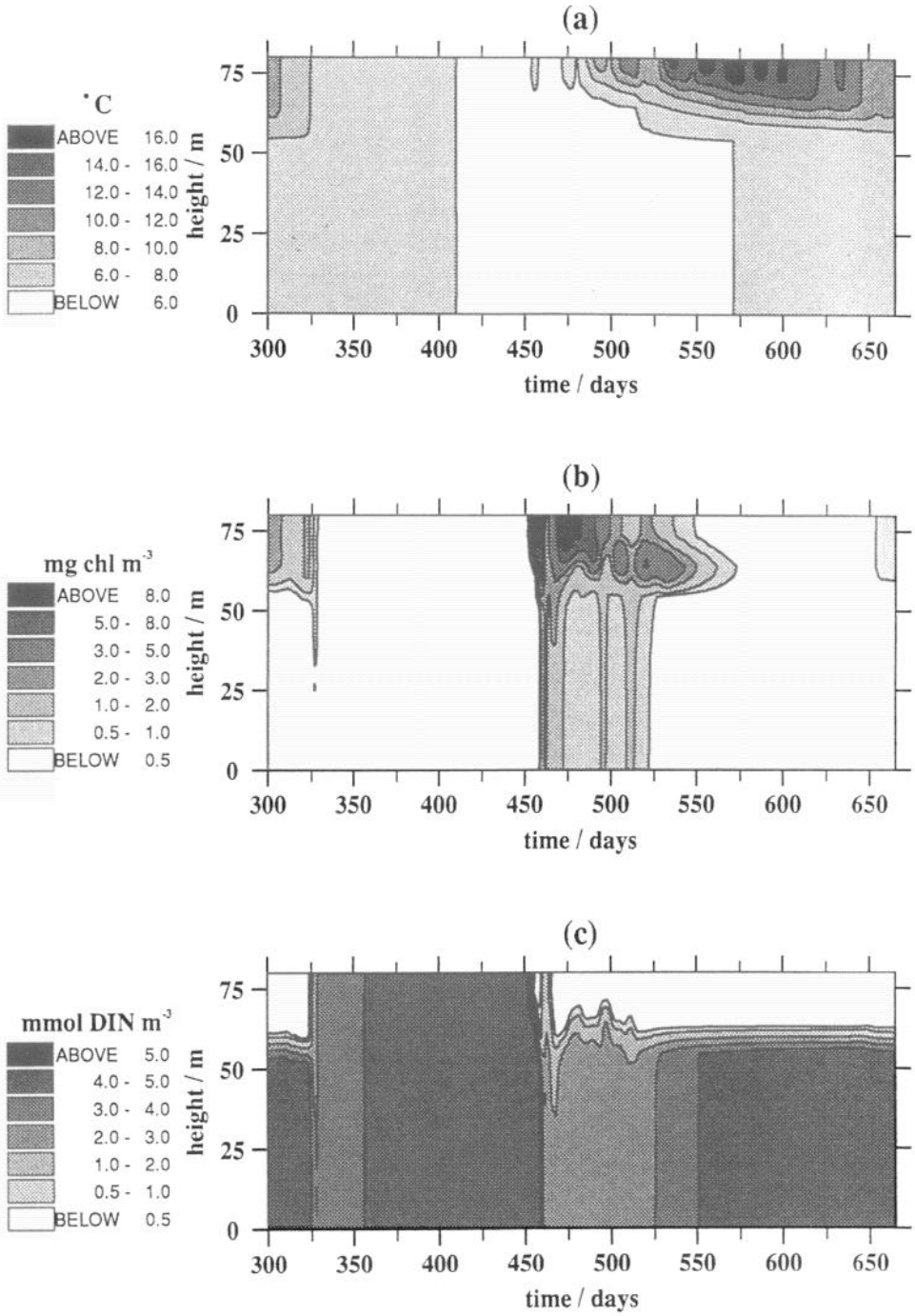

Figure 6. Model results under the conditions of station CS (run 3: daily meteorology). Height (meters) versus time (days from January 1st 1988) contours of: (a) temperature (°C); (b) biomass (mg chl m^{-3}); (c) DIN (mmol DIN m^{-3}).

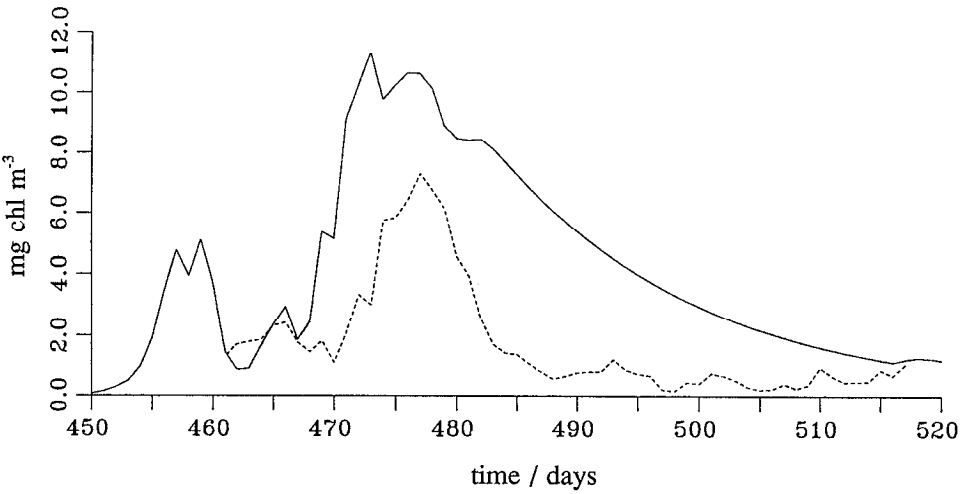

Figure 7. Comparison between modelled and observed near-surface chlorophyll during a mooring deployment at station CS. The solid line is the model prediction, the dotted line is that measured by a moored recording fluorometer.

the modelled DIN to help interpretation. Data were output at daily intervals, and so are not restricted temporally in contrast with the C.T.D. data. Figure 7 shows the comparison between the near surface measurements of chlorophyll from the moor-ing and the model output. A modelled spring bloom of about approximately 10 mg chl m^{-3} occurs at the start of the stratified period, with a short-lived initial pulse about day 457 (April 2nd) and a main peak about day 475 (April 20th). The pattern is similar to that shown by the recording fluorometer, although there are differences in detail.

By using more realistic meterological inputs, in particular a more variable wind stress, rather than the smoothly varying seasonal sinusoids of the previous section the model run for Figure 6 does not require any background mixing to produce mid-water chlorophyll structure. Figure 6 also shows the modelled thermocline to be closer to the surface than is the case in the observations. Consequentially, PAR levels predicted for the model thermocline are higher than those reaching the observed thermocline. The result in the model is to allow a greater rate of photosynthetic formation of biomass for a given vertical nitrogen flux and could explain why the mid-water modelled chlorophyll maximum is stronger than that observed.

Despite the simplicity of the biological model it is still dependent on the 14 empirically determined constants listed in Table 1. In particular the zooplankton grazing impact on the phytoplankton will be expected to have some seasonal variation, while on shorter timescales it may also vary with the level of turbulence in the water column. For instance either decreasing the grazing impact rate, g, toward zero, or increasing the recycled proportion of grazed nutrient, e, toward 1.0 will

Table 3. Dynamics of the midwater chlorophyll maximum at the time of the C.T.D. cast on day 547 (July 1st 1989) for the 3 model runs and the observations.

	Run 1	Run 2	Run 3	Observed
Depth of maximum chlorophyll (m)	22	18	18	33
Contribution to water column chl (excess over background mg chl m^{-2})	0.1	20	9	10
Background eddy diffusivity ($m^2 s^{-1}$)	0	1.0×10^{-5}	0	?
$\Delta S/\Delta z$ (mmol N m^{-4})	1.3	0.9	—	—
$\Delta h/\Delta t$ (m d^{-1})	—	—	0.1	0.05
S_{tm} (mmol N m^{-3})	—	—	4.0	2.1
DIN flux (mmol N $m^{-2} d^{-1}$)	0	0.8	0.4	0.1
Contribution of DIN flux to chl (mg chl $m^{-2} d^{-1}$)	0	1.3	0.7	0.2
Growth rate allowed by DIN flux (d^{-1}, assuming (0.5 new)/ (new + recycled) nitrogen)	0	0.13	0.15	0.04

prolong the existence of any mid-water chlorophyll structure without the need for any residual diapycnal mixing. There is, therefore, considerable scope for investigation into the model response to changes in the empirical parameters, though in the context of the effect of physical variability we have chosen to use fixed values for all parameters based on reliable observational evidence.

7. Dynamics of the midwater chlorophyll maximum

Table 3 gives estimates of vertical DIN flux into the bottom of the zone of the midwater chlorophyll maximum at or about day 185. For model runs 1 and 2 the flux is calculated from $-K_z(\partial S/\partial z)$, in the other cases from $-(\partial h/\partial t)S_{tm}$ where $\partial h/\partial z$ gives the rate of change of depth of an appropriate isotherm and S_{tm} is the DIN concentration in the tide-mixed layer. In the case of run 2, it appears that a vertical flux of 0.8 mmol N $m^{-2} d^{-1}$ is needed to sustain the midwater chlorophyll maximum which contributes an excess of about 20 mg chl m^{-2} to column total chlorophyll. With a local cell quota of 0.6 mmol N (mg chl)$^{-1}$, this vertical flux of new nitrogen would support a growth rate of 0.07 d^{-1}. Since recycling by zooplankton excretion can also provide much of the nitrogen required by plankton, the actual growth rate is likely to be close to the grazing pressure of 0.12 d^{-1} imposed by the model and implies that the model will be sensitive to the parameters g and e.

Such a calculation suggests that the midwater chlorophyll maximum is a steady state phenomenon, with the constant but small diapycnal flux of new nitrogen, driven by the background diffusivity, balancing non-recycled losses to zooplankton grazing and by weak diffusion of phytoplankton out of the thermocline. The results of run 3, using "real" weather, point, however, to an intermittent entrainment mechanism drive by variability in the surface wind stress, with the consequence that the midwater

chlorophyll maximum will exist continuously throughout the summer only if the time between entrainment events is less than the utilization timescale of the nitrogen they introduce into the system.

8. Conclusions

Existing physical and biological models have been successfully coupled together, forming a more complete model of the water column that allows direct dependence of the phytoplankton on the locally evolving physics. The link between the physics and the biology is principally through the modelling of vertical turbulent diffusivities as functions of local stability, and using them in the depth and time-dependent process equations for the biological parameters. This calculation of K_z as a result of the physical driving forces removes both the requirement of using time and depth invariant diffusivities from observations, and the simplification of a 2 or 3 layer approach of earlier biological models. The combined model thus provides a useful framework upon which to test hypotheses concerning biological and physical-biological interactions.

The comparison between model and observations over a seasonal cycle suggests satisfactory general agreement, and highlights two important points.

First, the earlier requirement of background mixing (see Section 4) appears to have been removed by using daily meterological inputs in place of smoothly varying seasonal averages. We suggest, therefore, that variability in the surface windstress is an important contribution to the formation of mid-water chlorophyll maxima by episodically weakening the thermocline barrier to nutrient input to the surface waters. This is a similar result to that of Klein and Coste (1984) who used a 1-d turbulence closure model of the ocean surface mixed layer in a study of nutrient entrainment through the thermocline. Inclusion of such meteorological variability on timescales of hours or even minutes may be required for a complete description of this stochastic process. Without knowledge of the high frequency meteorological variations a background diffusivity can be used as a mean representation of this variability.

Second, the thermal structure produced by the model differs from that observed, suggesting that either the closure scheme is underestimating the effect of windstress at the surface or that horizontal advection in the North Sea plays a significant role in the seasonal heat cycle. The large vertical temperature gradients produced by the model compared to the observations may also indicate the existence of other mixing processes at the thermocline that are not accounted for in the boundary-layer approach of the turbulence closure scheme, such as internal waves. The breaking of internal waves at the thermocline is effectively a random process often represented in terms of a background eddy viscosity and diffusivity (e.g. Veronis, 1969; Mellor and Durbin, 1975).

Our main conclusion on the basis of the above discussion is that it is likely that an important contribution to the biological and physical environment is random variability in the inputs to the system. The modelling suggests that the mid-water chlorophyll maximum is the result of episodes of nutrient flux into the thermocline, caused by pulses in the strength of the mixing processes. This will be in addition to any depth-dependence of the algal chlorophyll to cellular nutrient ratio. Such variability alters both the vertical position and internal structure of the thermocline, and in the absence of adequate observations has to be described in terms of background eddy coefficients. However, both meteorological variability and background eddy coefficients are likely to be required for a complete description of wind-driven and internal wave entrainment of nutrient through the thermocline.

Acknowledgments. Jonathan Sharples was supported by EC MAST-I-0050, and the North Sea data were obtained as part of the North Sea Community Project which included NERC GST/02/268 to Paul Tett.

REFERENCES

Chen, D., S. G. Horrigan and D.-P. Wang. 1988. The late summer vertical nutrient mixing in Long Island Sound. J. Mar. Res., *46,* 753–770.

Edinger, J. E., D. W. Duttweiler and J. C. Geyer. 1968. The response of water temperatures to meterological conditions. Water Res. Res., *4,* 1137–1145.

Fasham, M. J. R., P. M. Holligan and P. R. Pugh. 1983. The spatial and temporal development of the spring phytoplankton bloom in the Celtic Sea, April, 1979. Prog. Oceanogr. *12,* 87–145.

Holligan, P. M. and D. S. Harbour. 1977. The vertical distribution and succession of phytoplankton in the western English Channel 1975 and 1976. J. Mar. Biol. Assoc. U.K., *57,* 1075–1093.

Howarth, M. J., K. R. Dyer and I. R. Joint. 1993. Seasonal cycles and their spatial variability. Phil. Trans. Royal Soc. London, *A340* (in press).

Jamart, B. M., D. F. Winter, K. Banse, G. C. Anderson and R. K. Lam. 1977. A theoretical study of phytoplankton growth and nutrient distribution in the Pacific Ocean off the northwestern U.S. coast. Deep-Sea Res., *24,* 753–773.

Kiefer, D. A. and J. N. Kremer. 1981. Origins of vertical patterns of phytoplankton and nutrients in the temperate, open ocean: a stratigraphic hypothesis. Deep-Sea Res., *28,* 1087–1105.

Klein, P. and B. Coste. 1984. Effects of wind-stress variability on nutrient transport into the mixed layer. Deep-Sea Res., *31,* 21–37.

Margalef, R. 1978. Life-forms of phytoplankton as survival alternatives in an unstable environment. Oceanol. Acta, *1,* 493–509.

Mellor, G. L. and P. A. Durbin. 1975. The structure and dynamics of the ocean surface mixed layer. J. Phys. Oceanogr., *5,* 718–728.

Mellor, G. L. and T. Yamada. 1974. A hierarchy of turbulence closure models for planetary boundary layers. J. Atmos. Sci., *31,* 1791–1806.

—— 1982. Development of a turbulence closure model for geophysical fluid problems. Rev. Geophys. Space Phys., *20,* 851–875.

Mills, D. K. and P. B. Tett. 1990. Use of a recording fluorometer for continuous measurement of phytoplankton concentration. SPIE Proceedings, *1269,* 106–115.

Mills, D. K., P. Tett and G. Novarino. 1993. The spring bloom in the south-western North Sea in 1989. Netherlands J. Sea Res., (in press).

Pingree, R. D., L. Maddock and E. I. Butler. 1977. The influence of biological activity and physical stability in determining the chemical distributions of inorganic phosphate, silicate and nitrate. J. Mar. Biol. Assoc. U. K., *57,* 1065–1073.

Press, W. H., B. P. Flannery, S. A. Teukolsky and W. T. Vetterling. 1986. Numerical Recipes: The Art of Scientific Computing. Cambridge University Press, 818 pp.

Simpson, J. H. and D. G. Bowers. 1984. The role of tidal stirring in controlling the seasonal heat cycle in shelf seas. Annales Geophysicae, *2,* 411–416.

Simpson, J. H., P. B. Tett, M. L. Argote-Espinoza, A. Edwards, K. J. Jones and G. Savidge. 1982. Mixing and phytoplankton growth around an island in a stratified sea. Cont. Shelf Res., *1,* 15–31.

Steele, J. H. and C. S. Yentsch. 1960. The vertical distribution of chlorophyll. J. Mar. Biol. Assoc. U.K., *39,* 217–226.

Taylor, A. H., J. R. W. Harris and J. Aiken. 1986. The interaction of physical and biological processes in a model of the vertical distribution of phytoplankton under stratification, *in* Marine Interfaces Hydrodynamics, J. C. J. Nihoul, ed., Elsevier Oceanography Series, *42,* Amsterdam. 313–330.

Tett, P. 1981. Modelling phytoplankton production at shelf-sea fronts. Phil. Trans. Roy. Soc. London, *A302,* 605–615.

—— 1987. Modelling the growth and distribution of marine microplankton, *in* Ecology of Microbial Communities, Cambridge University Press, 387–425.

Tett, P., A. Edwards and K. Jones. 1986. A model for the growth of shelf-sea phytoplankton in summer. Estuar. Coastal and Shelf Sci., *23,* 641–672.

Tett, P., I. Joint, D. Purdie, M. Baars, S. Oosterhuis, G. Daneri, F. Hannah, D. K. Mills, D. Plummer, A. Pomroy, A. W. Walne and H. J. Witte. 1993. Biological consequences of tidal mixing gradients in the North Sea. Phil. Trans. Roy. Soc. London, *A340,* 493–508.

Varela, R. A., A. Cruzado, J. Tintoré and E. G. Ladona. 1992. Modelling the deep-chlorophyll maximum: a coupled physical-biological approach. J. Mar. Res. *50,* 441–463.

Veronis, G. 1969. On theoretical models of the thermocline circulation. Deep-Sea Res., *16,* (Suppl.), 301–323.

Walters, R. A. 1980. A time- and depth-dependent model for physical, chemical and biological cycles in template lakes. Ecol. Model., *8,* 79–96.

Woods, E. A. and P. B. Tett. 1994. Predicting the distribution and seasonal cycle of phytoplankton on the Malin shelf, Scotland, using a two layer model for tidally stirred shelf seas. Estuar. Coastal Shelf Sci., (submitted).

Received: *4 May, 1993;* revised: *7 October, 1993.*